PROCEEDINGS OF SPIE

SPIEDigitalLibrary.org/conference-proceedings-of-spie

Long-term, super-resolution imaging of amyloid structures using transient amyloid binding microscopy

Tianben Ding, Kevin Spehar, Jan Bieschke, Matthew D. Lew

Tianben Ding, Kevin Spehar, Jan Bieschke, Matthew D. Lew, "Long-term, super-resolution imaging of amyloid structures using transient amyloid binding microscopy," Proc. SPIE 10884, Single Molecule Spectroscopy and Superresolution Imaging XII, 108840J (22 February 2019); doi: 10.1117/12.2507656



Event: SPIE BiOS, 2019, San Francisco, California, United States

Long-term, super-resolution imaging of amyloid structures using transient amyloid binding microscopy

Tianben Ding^a, Kevin Spehar^b, Jan Bieschke^c, and Matthew D. Lew*^a

^aDepartment of Electrical and Systems Engineering, Washington University in St. Louis,

1 Brookings Drive, St. Louis, MO, USA 63130

^bDepartment of Biomedical Engineering, Washington University in St. Louis,

1 Brookings Drive, St. Louis, MO, USA 63130

^cMRC Prion Unit, UCL Institute of Prion Diseases, 33 Cleveland St., London, W1W 7FF, UK

ABSTRACT

Amyloid fibrils and tangles are signatures of Alzheimer disease, but nanometer-sized aggregation intermediates are hypothesized to be the structures most toxic to neurons. The structures of these oligomers are too small to be resolved by conventional light microscopy. We have developed a simple and versatile method, called transient amyloid binding (TAB), to image amyloid structures with nanoscale resolution using amyloidophilic dyes, such as Thioflavin T, without the need for covalent labeling or immunostaining of the amyloid protein. Transient binding of ThT molecules to amyloid structures over time generates photon bursts that are used to localize single fluorophores with nanometer precision. Continuous replenishment of fluorophores from the surrounding solution minimizes photobleaching, allowing us to visualize a single amyloid structure for hours to days. We show that TAB microscopy can image both the oligomeric and fibrillar stages of amyloid- β aggregation. We also demonstrate that TAB microscopy can image the structural remodeling of amyloid fibrils by epi-gallocatechin gallate. Finally, we utilize TAB imaging to observe the non-linear growth of amyloid fibrils.

Keywords: Single-molecule localization microscopy, amyloid-beta peptides, amyloid aggregation, binding-activated fluorescence

1. INTRODUCTION

Amyloids, aggregates of misfolded short proteins, cause various aging-related human diseases, such as Alzheimer disease (AD) and Parkinson disease. The 42 amino-acid residue amyloid-beta peptide (A β 42) forms extracellular plaques in the brains of AD patients that are a pathological signature of the disease. Protein misfolding and fibril formation from monomeric structures are unique characteristics of amyloids including A β 42, and nanometer-sized aggregation intermediates, termed oligomers, are typically considered to be the most toxic structures. ^{1–3} Amyloid aggregation, including the formation of oligomers, is dynamic, transitory, and heterogeneous, and its mechanisms are still not fully understood. A new imaging methodology with single-molecule sensitivity and long-term measurement capability is required for quantitatively studying the nanometer-scale inhomogeneities and dynamics of the aggregates.

Conventional fluorescence microscopy is ubiquitous in studies of dynamics in living systems due to its specificity from its molecular tags and its relatively non-invasive nature from its use of non-ionizing radiation. However, the physical resolution barrier, optical diffraction, bounds its resolution to approximately 250 nm given by the Abbe diffraction limit $\lambda/2NA$. Single-molecule (SM) super-resolution (SR) fluorescence microscopy techniques, such as (f)PALM^{5,6} and (d)STORM,^{7,8} overcome this physical limitation by actively switching densely labeled molecules between bright and dark states to reduce the concentration of emitters within a sample. The states of molecules can be switched by using a variety of mechanisms including photoactivation and chemical-induced photoswitching.^{9,10} A SR image can be reconstructed by recording these "blinking" events and localizing each bright molecule with nanoscale precision.¹¹

Single Molecule Spectroscopy and Superresolution Imaging XII, edited by Zygmunt Karol Gryczynski, Ingo Gregor, Felix Koberling, Proc. of SPIE Vol. 10884, 108840J ⋅ © 2019 SPIE CCC code: 1605-7422/19/\$18 ⋅ doi: 10.1117/12.2507656

^{*}mdlew@wustl.edu; phone 1-314-935-6790; fax 1-314-935-7500; lewlab.wustl.edu

We have developed a SR imaging technique to visualize amyloid structures on the nanometer scale, called Transient Amyloid Binding (TAB) imaging.¹² Instead of covalent attachment¹³ or permanent intercalation¹⁴ of fluorophores, TAB imaging uses transient binding of standard amyloidophilic dyes to amyloid structures. Amyloidophilic dyes, such as Thioflavin T (ThT), specifically bind to crossed β -sheets that form the fibrillar backbone and increase their quantum yield upon binding.¹⁵ The molecules emit fluorescence until they dissociate from the structure or photobleach. We record "blinking" of ThT molecules, localize their positions on amyloids with nanometer precision, and reconstruct the underlying structures. Our method is similar in concept to PAINT, which was first demonstrated for imaging lipid bilayers using Nile red as an imaging probe.¹⁶

In this proceeding, we demonstrate a key advantage of TAB imaging, namely its long-term imaging capability relative to traditional super-resolution techniques, and show its suitability for studying dynamics of amyloid structures. We also show the use of Nile red as a TAB imaging probe for long-term observation of fibril growth.

2. METHODS

Unless stated otherwise, all chemicals were purchased from Sigma-Aldrich and are ACS grade.

2.1 Amyloid Preparation

 $A\beta42$ peptide purchased from ERI Amyloid Laboratory was dissolved in hexafluoro-2-propanol (HFIP), and sonicated at room temperature for one hour in a water bath sonicator. After freezing in liquid nitrogen, HFIP was removed by lyophilization, and aliquots of the peptide were stored at -20 °C. To prepare amyloid aggregates, lyophilized $A\beta42$ were dissolved in 10 mM NaOH, sonicated for 25 min in a cold water bath, and filtered first through a 0.2 μ m and then through a 30 kD centrifugal membrane filter (Millipore) as described previously. ¹⁷ To prepare fibrils, we incubated 10 - 50 μ M monomeric $A\beta42$ in PBS (150 mM NaCl, 50 mM Na₃PO₄, pH 7.4) at 37 °C with 200 rpm shaking for 24 hours. Fibril formation was verified by an atomic force microscope. To prepare oligomers, we incubated 10 - 50 μ M monomeric $A\beta42$ in Dulbecco's Modified Eagle Medium (DMEM)/Nutrient Mixture F-12 (ThermoFisher Scientific) at 4 °C without agitation for 24 hours. Oligomeric structures were also verified by an atomic force microscope.

2.2 Imaging Sample Preparation

Eight-well cell culture chambers with glass coverslip bottoms (Lab Tek, No. 1.5H, 170 \pm 5 μ m thickness) were cleaned using a UV Ozone Cleaner (Novascan Technologies) for 15 minutes. Amyloid solutions were prepared as described in section 2.1. A solution containing amyloid aggregates (10 μ L) was adsorbed to the coverslip for 1 hour. The coverslip was rinsed with 200 μ L dH₂O afterward.

2.3 Imaging Procedure

TAB images were captured as follows. A PBS solution (200 μ L) containing 1 μ M ThT or 500 nM Nile red (Fisher Scientific) was placed into the amyloid-adsorbed chambers. Super-resolution imaging was performed on a home-built microscope¹² equipped with an oil-immersion objective (Olympus, 100X, 1.4 NA) and a 488 nm or a 561 nm excitation laser for exciting ThT or Nile red, respectively. The peak intensities of the lasers at the sample were 1.8 kW/cm² for the 488 nm and 0.45 kW/cm² for the 561 nm lasers. Stacks of 5,000 images with 20 ms camera exposure were recorded for each TAB reconstruction.

Time-lapse imaging of amyloid remodeling was captured as follows. A β 42 fibrils were adsorbed to ozone-cleaned chambers (section 2.1). epi-gallocatechin gallate (EGCG, Taiyo International) was added to an imaging buffer in the amyloid-adsorbed chambers in order to remodel and dissolve amyloid fibrils. After variable-length incubations as indicated in Fig. 3 in the presence of 1 mM EGCG at room temperature (21 °C), the sample was rinsed and replaced with the ThT imaging buffer for TAB imaging. This procedure was repeated over 46 hours.

Time-lapse imaging of amyloid elongation was captured as follows. A β 42 fibrils were needle sheared by pulling through a 25G needle ten times to form short seeds.¹⁹ The seed sample was then adsorbed onto an ozone-cleaned coverslip (Azer Scientific, No. 1.5H, 170 \pm 5 μ m thickness) as described in section 2.1. A solution (10 μ L) containing 20 μ M monomeric A β 42 and 500 nM Nile red in PBS was placed onto the coverslip. The solution was sandwiched by another coverslip from the top and sealed with wax to prevent evaporation. The

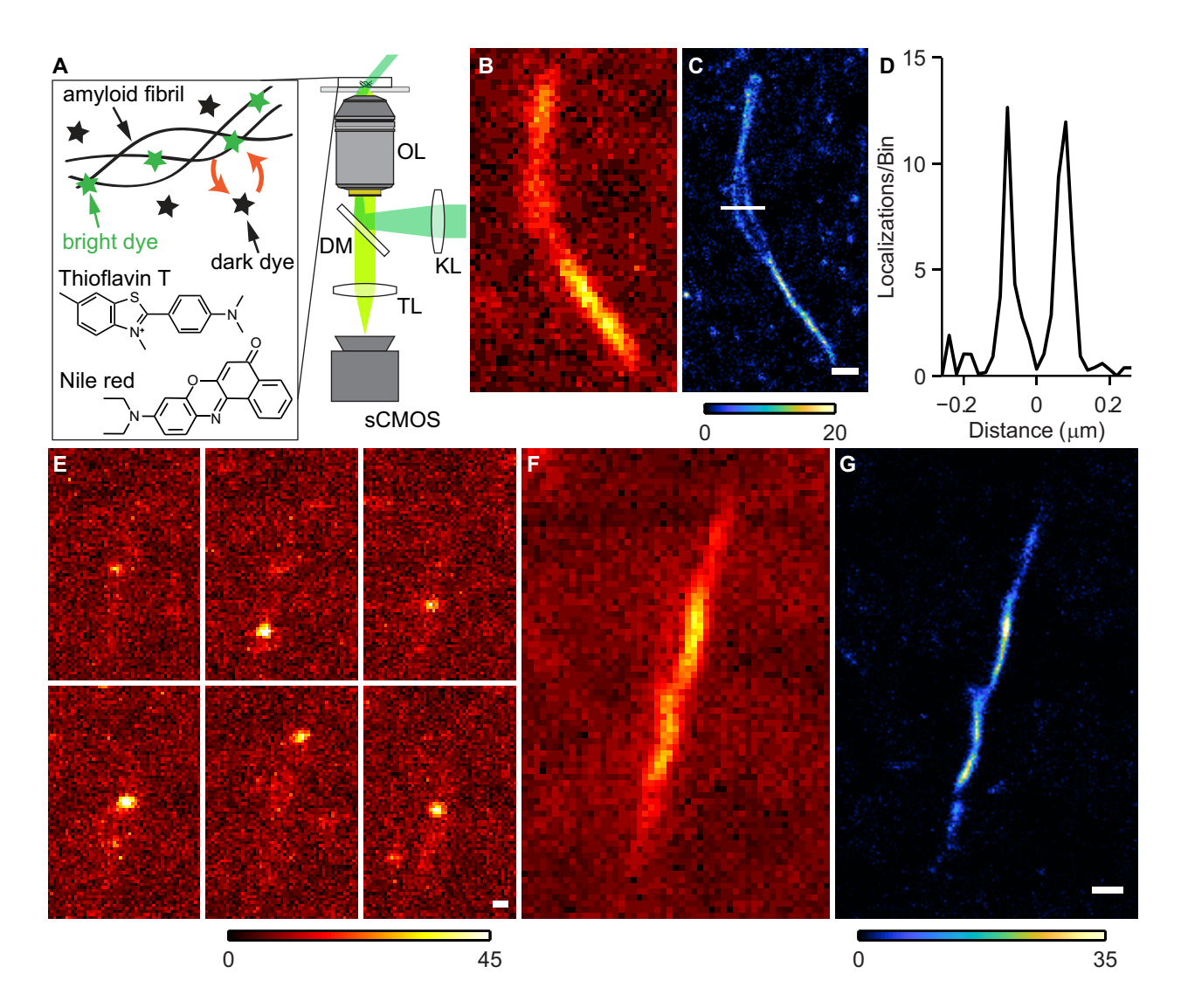


Figure 1. Transient amyloid binding microscopy. A) Inclined laser illumination excites fluorophores transiently bound to amyloid structures, and collected fluorescence is captured by an sCMOS camera. KL: widefield lens, OL: objective lens, DM: dichroic mirror, TL: tube lens. Inset: transient binding, fluorescence activation, and unbinding of amyloidophilic dyes and the chemical structures of Thioflavin T (ThT) and Nile red. B) Diffraction-limited image using Nile red of an A β 42 fibril. C) Nile red TAB SR image of the fibril in (B). Color scale: localizations per bin. D) Cross-section of the white line across the fibril in (C). E) ThT blinking on another A β 42 fibril. Color scale: photons per pixel. F) Diffraction-limited imaging using ThT of the fibril in (E). G) ThT TAB SR image of the A β 42 fibril in (E, F). Color scale: localizations per bin. Scale bars: 300 nm.

sample was incubated on our microscope stage at room temperature (21 °C) without changing any buffers and meanwhile, Nile red TAB imaging was performed periodically over 21 hours.

The captured image stacks were offset-corrected at each pixel by subtracting an averaged dark image. The images where then localized using the ThunderSTORM²⁰ plugin within ImageJ using default settings and custom camera parameters. Further post-processing was performed using MATLAB (Mathworks, R2018a) for calculating localization precision and reconstructing SR images as previously described.¹²

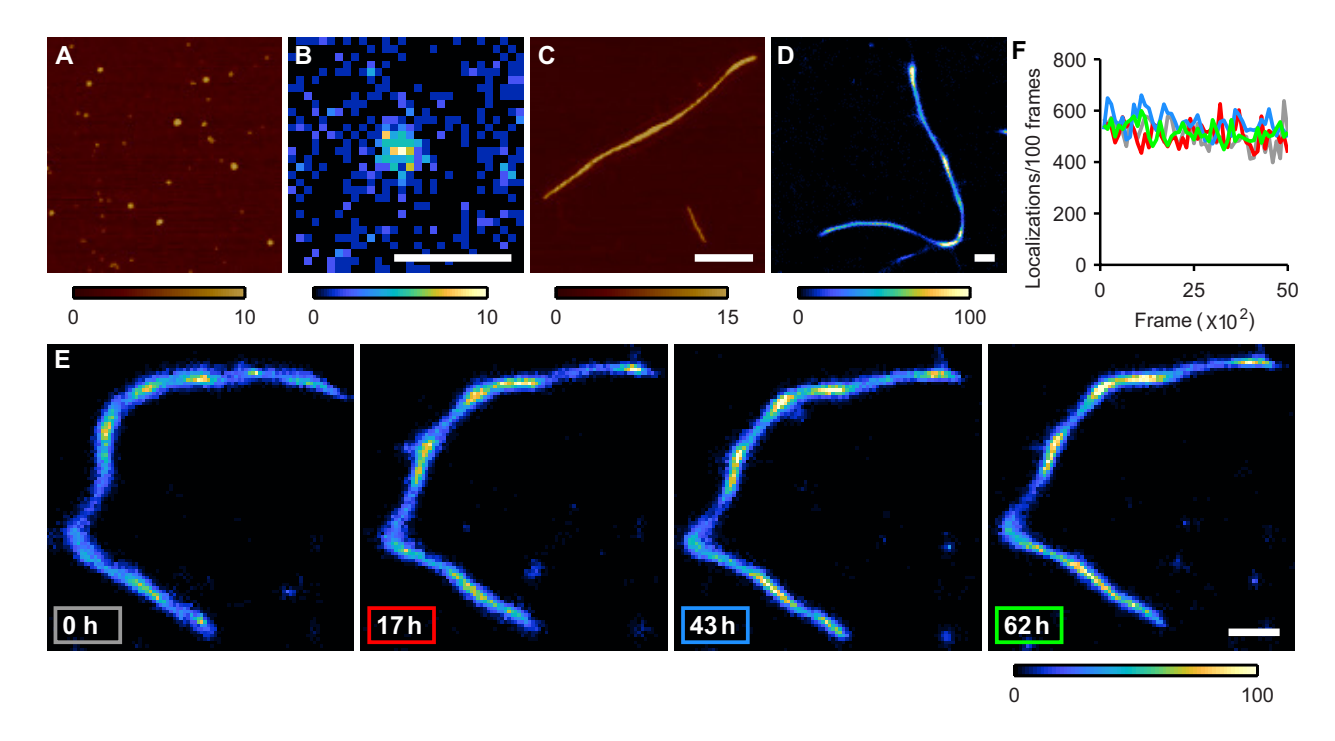


Figure 2. $A\beta42$ structures at different aggregation stages and TAB images over extended observation times of an $A\beta42$ fibril. A, C) AFM images of $A\beta42$ A) origomers and C) fibrils. Color bars in nm. B, D) TAB images of an $A\beta42$ B) origomer and D) fibril using ThT. Color scale: localizations per bin. E) Time-lapse Nile red TAB imaging of an $A\beta42$ fibril. Color scale: localizations per bin. Scale bars: 300 nm. F) Localization rates during the acquisition of image stacks for the Nile red TAB images shown in (E). 0 h in gray, 17 h in red, 43 h in blue, and 62 h in green lines.

3. RESULTS AND DISCUSSION

In order to demonstrate the concept of TAB imaging, we imaged $A\beta42$ fibrils adsorbed to an imaging chamber using an epi-fluorescence microscope with an inclined excitation laser (Fig. 1A). In addition to ThT, we also used Nile red as a TAB probe in this work. The binding affinity of Nile red to amyloid structures has been used to map the hydrophobicity of amyloid structures. The image sequence (Fig. 1E) shows the blinking of single ThT molecules on an amyloid fibril. SR images with a 20×20 nm² bin size were reconstructed by localizing multiple blinking events of Nile red (Fig. 1C) or ThT (Fig. 1G) as described in section 2.3. The SR images show the improvement of image resolution (FWHM: 47 nm by ThT, 35 nm by Nile red) over that in the diffraction-limited (DL) images (Figs. 1BF) of the same structures. Our signal-to-background ratio allows TAB to achieve 15 nm (ThT) and 9 nm (Nile red) localization precisions. TAB SR imaging reveals twisting fibrillar structural details that cannot be resolved in the conventional DL image (Fig. 1D).

We next explored whether TAB imaging could visualize smaller aggregation intermediates along the pathway of amyloid aggregation. Our preparations of origomer and fibril structures (Section 2.1) were verified by atomic force microscopy (AFM, Figs. 2AC). We performed TAB imaging of the A β 42 aggregates using ThT as the probe. TAB imaging was able to reconstruct spherical A β 42 origomers (Fig. 2B) although with fewer localizations than that on fibril structures (Fig. 2D).

To image the dynamics of amyloid formation, it is essential to have a robust tool that can follow the structure of a single aggregate over hours or days. We analyzed the stability of TAB imaging by testing whether the localization number and reconstruction quality remained constant over extended observation times. We imaged an A β 42 fibril 4 times over 62 hours using Nile red as the probe. We observed that the TAB reconstructions (Fig. 2E) and the rate of localizations in each 5000-frame stack (100 s image stack acquisition with 20 ms exposure time, Fig. 2F) remained approximately constant over the 62-hour acquisition. Therefore, TAB imaging with Nile red is robust against photobleaching and capable of producing multiple time-lapse SR images. TAB's robustness

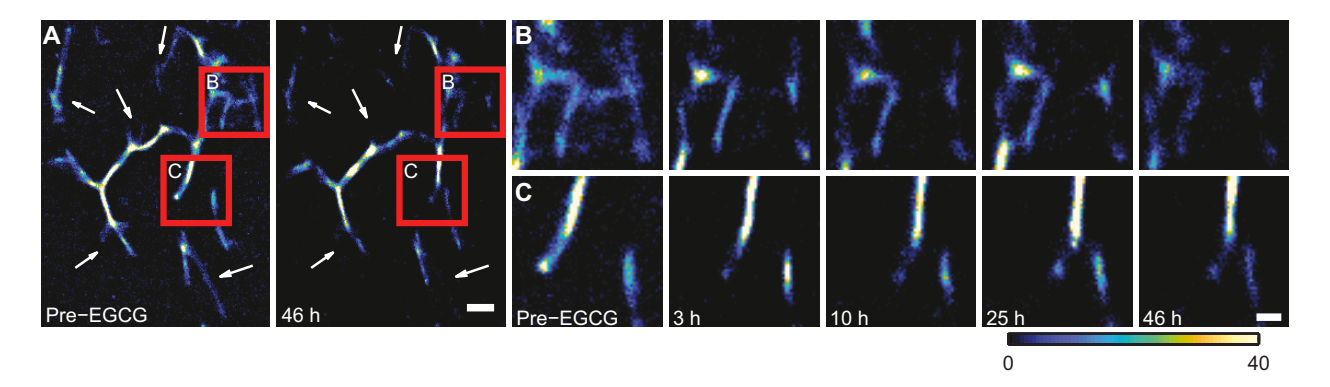


Figure 3. TAB SR images of $A\beta42$ fibril remodeling using ThT as the imaging probe. A) $A\beta42$ before and after a 46-hour reaction with EGCG (1 mM). White arrows denote regions with distinct changes. Scale bar: 500 nm. B, C) Time-lapse TAB images of regions denoted by red squares in (A), recorded before and 3, 10, 25, and 46 h after adding EGCG. Color bar denotes localizations per bin, scale bar: 200 nm. Reprinted with permission from Ref. 12.

against photobleaching using ThT has been validated previously.¹² These results also demonstrate that both ThT and Nile red only bind transiently to amyloid structures, thereby allowing new molecules from solution to continuously sample the same binding sites over hours and even days.

Next, we imaged two types of amyloid dynamics by utilizing the long-term imaging capability of TAB. The time-lapse images of ThT TAB (Fig. 3) show the dissolution and remodeling of A β 42 fibrils by epi-gallocatechin gallate (EGCG). Remarkably, TAB imaging captured the structural dynamics of amyloid fibrils over 2 days, allowing us to observe remodeling over tens of micrometers with nanometer localization precision. We also imaged amyloid elongation on our microscope stage using Nile red TAB imaging. The time-lapse TAB images (Fig. 4) show non-linear growth of amyloid fibrils over time that cannot be clearly resolved in the corresponding DL images. TAB's robustness against photobleaching allowed us to observe transitions between active elongation and arrested growth with nanoscale resolution.

4. CONCLUSION

In this proceeding, we demonstrated TAB SR imaging using two amyloidophilic dyes, ThT and Nile red. Our SR images, collected over hours to days, show TAB imaging's suitability for longitudinal study of the dynamics of amyloid structures with nanoscale resolution. In addition, TAB imaging uses standard amyloid dyes without the need for covalent modification of the amyloid protein or immunostaining. Moreover, the transient labeling strategy reduces complexity of sample preparation and allows us to minimize the perturbation of amyloid structures and dynamics during imaging. These capabilities will make TAB imaging broadly useful across a variety of amyloid and amyloid-disease-related studies in the future.

ACKNOWLEDGMENTS

Research reported in this publication was supported by the National Science Foundation under grant no. ECCS-1653777 to M.D.L, by the National Institute of General Medical Sciences of the National Institutes of Health under grant no. R35GM124858 to M.D.L., and the Hope Center for Neurological Disorders pilot through a grant to J.B. The authors thank Yuanzi Sun and Niraja Kedia for technical assistance.

REFERENCES

[1] Harper, J. D. and Lansbury, P. T., "Models of amyloid seeding in Alzheimer's disease and scrapie: Mechanistic Truths and Physiological Consequences of the Time-Dependent Solubility of Amyloid Proteins," *Annual Review of Biochemistry* **66**, 385–407 (1997).

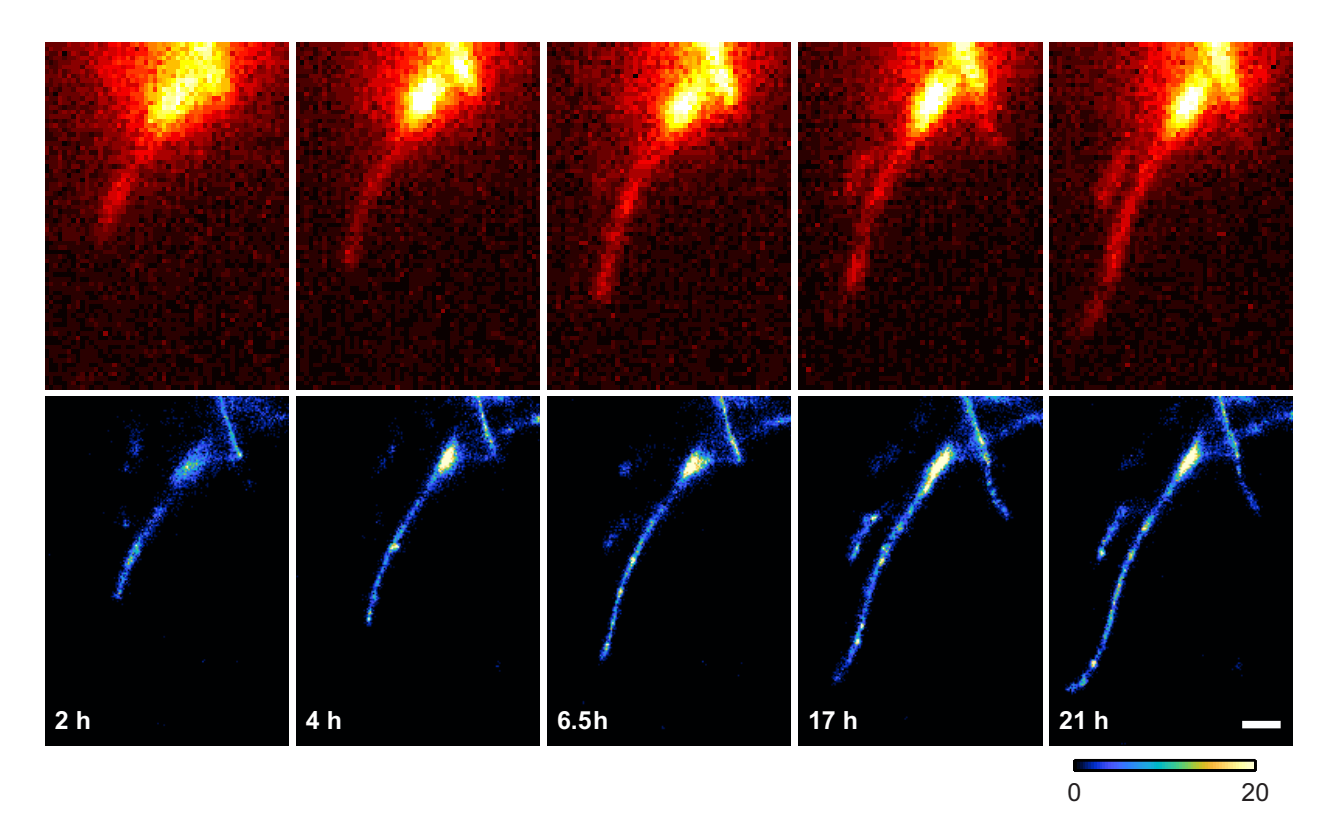


Figure 4. TAB SR images using Nile red of A β 42 fibril growth, recorded 2, 4, 6.5, 17, and 21 hours after placing the sample on our microscope stage at room temperature (21 °C). Top row: diffraction-limited images. Bottom row: corresponding TAB SR images. Color bar denotes localizations per bin. Scale bar: 300 nm.

- [2] Cohen, E., Bieschke, J., Perciavalle, R. M., Kelly, J. W., and Dillin, A., "Opposing Activities Protect Against Age-Onset Proteotoxicity," *Science* **313**, 1604–1610 (2006).
- [3] Iadanza, M. G., Jackson, M. P., Hewitt, E. W., Ranson, N. A., and Radford, S. E., "A new era for understanding amyloid structures and disease," *Nature Reviews Molecular Cell Biology* 19, 755–773 (2018).
- [4] Abbe, E., "Contributions to the theory of the microscope and microscopic detection," Arch. Mikroskop. Anat. 9, 413–418 (1873).
- [5] Betzig, E., Patterson, G. H., Sougrat, R., Lindwasser, O. W., Olenych, S., Bonifacino, J. S., Davidson, M. W., Lippincott-Schwartz, J., and Hess, H. F., "Imaging Intracellular Fluorescent Proteins at Nanometer Resolution," *Science* 313, 1642–1645 (2006).
- [6] Hess, S. T., Girirajan, T. P. K., and Mason, M. D., "Ultra-high resolution imaging by fluorescence photoactivation localization microscopy.," *Biophysical journal* 91, 4258–72 (2006).
- [7] Rust, M. J., Bates, M., and Zhuang, X. W., "Sub-diffraction-limit imaging by stochastic optical reconstruction microscopy (STORM)," *Nat Methods* **3**(10), 793–795 (2006).
- [8] Heilemann, M., van de Linde, S., Schüttpelz, M., Kasper, R., Seefeldt, B., Mukherjee, A., Tinnefeld, P., and Sauer, M., "Subdiffraction-Resolution Fluorescence Imaging with Conventional Fluorescent Probes," Angewandte Chemie International Edition 47, 6172–6176 (2008).
- [9] Ha, T. and Tinnefeld, P., "Photophysics of Fluorescent Probes for Single-Molecule Biophysics and Super-Resolution Imaging," *Annual Review of Physical Chemistry* **63**, 595–617 (2012).
- [10] Li, H. and Vaughan, J. C., "Switchable Fluorophores for Single-Molecule Localization Microscopy," Chemical Reviews 118, 9412–9454 (2018).

- [11] Sage, D., Kirshner, H., Pengo, T., Stuurman, N., Min, J., Manley, S., and Unser, M., "Quantitative evaluation of software packages for single-molecule localization microscopy," *Nature Methods* 12, 717–724 (2015).
- [12] Spehar, K., Ding, T., Sun, Y., Kedia, N., Lu, J., Nahass, G. R., Lew, M. D., and Bieschke, J., "Super-resolution Imaging of Amyloid Structures over Extended Times by Using Transient Binding of Single Thioflavin T Molecules," *ChemBioChem* 19, 1944–1948 (2018).
- [13] Kaminski Schierle, G. S., van de Linde, S., Erdelyi, M., Esbjorner, E. K., Klein, T., Rees, E., Bertoncini, C. W., Dobson, C. M., Sauer, M., and Kaminski, C. F., "In Situ Measurements of the Formation and Morphology of Intracellular β-Amyloid Fibrils by Super-Resolution Fluorescence Imaging," Journal of the American Chemical Society 133, 12902–12905 (2011).
- [14] Shaban, H. A., Valades-Cruz, C. A., Savatier, J., and Brasselet, S., "Polarized super-resolution structural imaging inside amyloid fibrils using Thioflavine T," Scientific Reports 7, 12482 (2017).
- [15] Biancalana, M. and Koide, S., "Molecular mechanism of Thioflavin-T binding to amyloid fibrils," *Biochimica et Biophysica Acta Proteins and Proteomics* **1804**(7), 1405–1412 (2010).
- [16] Sharonov, A. and Hochstrasser, R. M., "Wide-field subdiffraction imaging by accumulated binding of diffusing probes.," Proceedings of the National Academy of Sciences of the United States of America 103, 18911–6 (2006).
- [17] Kedia, N., Almisry, M., and Bieschke, J., "Glucose directs amyloid-beta into membrane-active oligomers," *Phys. Chem. Chem. Phys.* **19**(27), 18036–18046 (2017).
- [18] Bieschke, J., Russ, J., Friedrich, R. P., Ehrnhoefer, D. E., Wobst, H., Neugebauer, K., and Wanker, E. E., "EGCG remodels mature α -synuclein and amyloid- β fibrils and reduces cellular toxicity," *Proceedings of the National Academy of Sciences* **107**, 7710–7715 (2010).
- [19] Young, L. J., Kaminski Schierle, G. S., and Kaminski, C. F., "Imaging $A\beta(142)$ fibril elongation reveals strongly polarised growth and growth incompetent states," *Phys. Chem. Chem. Phys.* **19**(41), 27987–27996 (2017).
- [20] Ovesný, M., Kížek, P., Borkovec, J., Švindrych, Z., and Hagen, G. M., "ThunderSTORM: A comprehensive ImageJ plug-in for PALM and STORM data analysis and super-resolution imaging," *Bioinformatics* 30(16), 2389–2390 (2014).
- [21] Lee, J.-E., Sang, J. C., Rodrigues, M., Carr, A. R., Horrocks, M. H., De, S., Bongiovanni, M. N., Flagmeier, P., Dobson, C. M., Wales, D. J., Lee, S. F., and Klenerman, D., "Mapping Surface Hydrophobicity of α-Synuclein Oligomers at the Nanoscale," Nano Letters 18, 7494–7501 (2018).